

Supporting Information for

“Absence of remote earthquake triggering within the Coso and Salton Sea geothermal production fields”

Qiong Zhang^{1,2}, Guoqing Lin¹, Zhongwen Zhan², Xiaowei Chen³, Yan Qin³, and Shimon Wdowinski^{1,4}

¹Department of Marine Geosciences, University of Miami, FL

²Seismological laboratory, California Institute of Technology, CA

³Geology and Geophysics, University of Oklahoma, OK

⁴Department of Earth and Environment, Florida International University, FL

Contents

1. Table S1
2. Figures S1 to S6

Table 1. Statistical analysis of seismicity rate change for six subareas outside the Coso geothermal field.

For each subarea, the Poissonian probability is calculated based on seismicity rate in the 30-day window following the Landers earthquake. The null hypothesis that the observed increased seismicity rate is random is rejected when the probability is less than 0.5.

Subarea	Poisson Probability
Coso Range	0.0102
Rose Valley	0.0139
Centennial Flat	0.0453
Wilson Canyon Fault	10^{-6}
Airport Fault Lake Zone1	0.0134
Airport Fault Lake Zone2	0.0101

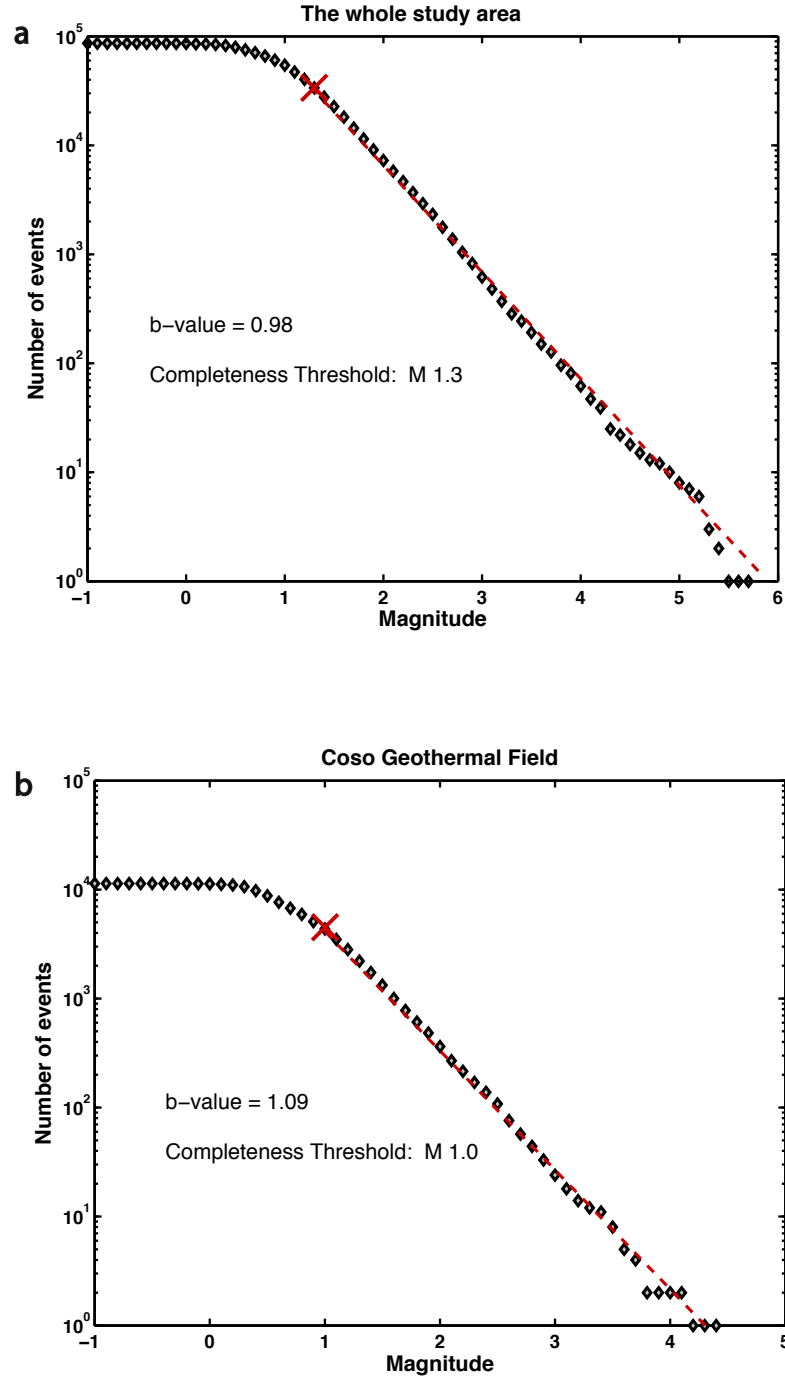


Figure 1. Estimate of catalog magnitude completeness and b -value for the entire study area (a) and the Coso geothermal field (b). The magnitudes of the largest earthquakes during our study period are Mw 5.75 and Mw 4.41 for the entire study area and the Coso Geothermal Field, respectively. Red crosses show the magnitude thresholds. The larger b -value inside the geothermal field than that for the entire study area indicates that the geothermal field is more dominated by events with smaller magnitudes.

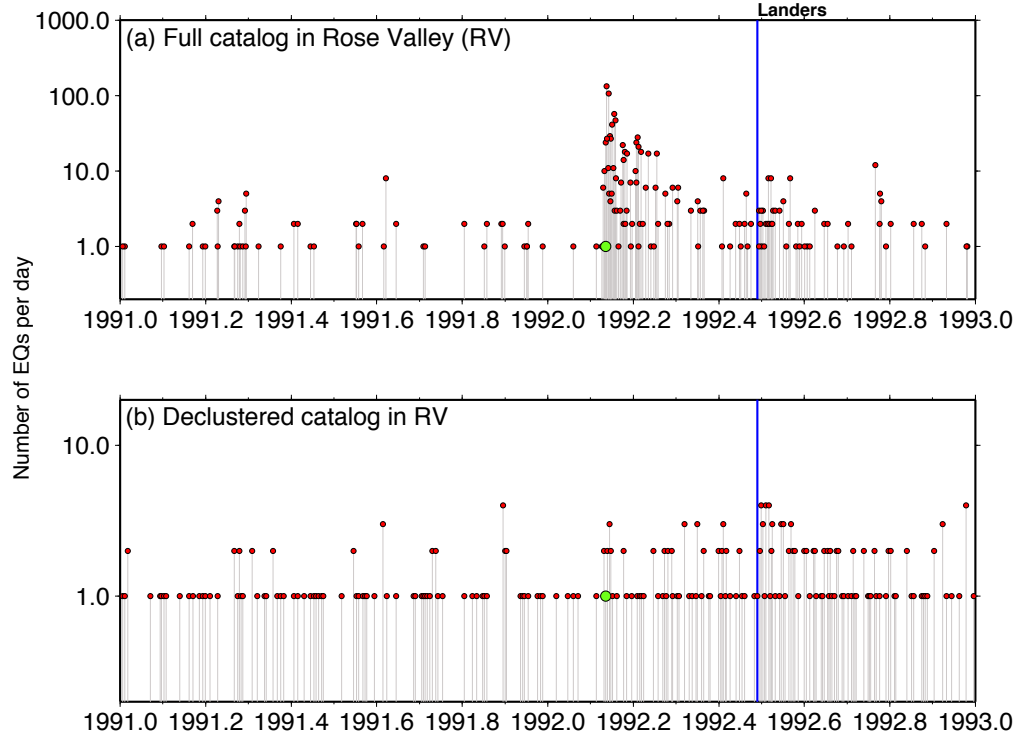


Figure 2. Example of catalog declustering in the Rose Valley (subarea 3). Red dots represent microearthquakes with $1.3 \leq M_w < 4.0$ and green dots denote the earthquakes with $M_w \geq 4.0$. Blue lines mark the onset of the Landers earthquake. (a) Time series of the full catalog, including a M_w 4.1 mainshock and its aftershock sequence. (b) Time series of the declustered catalog.

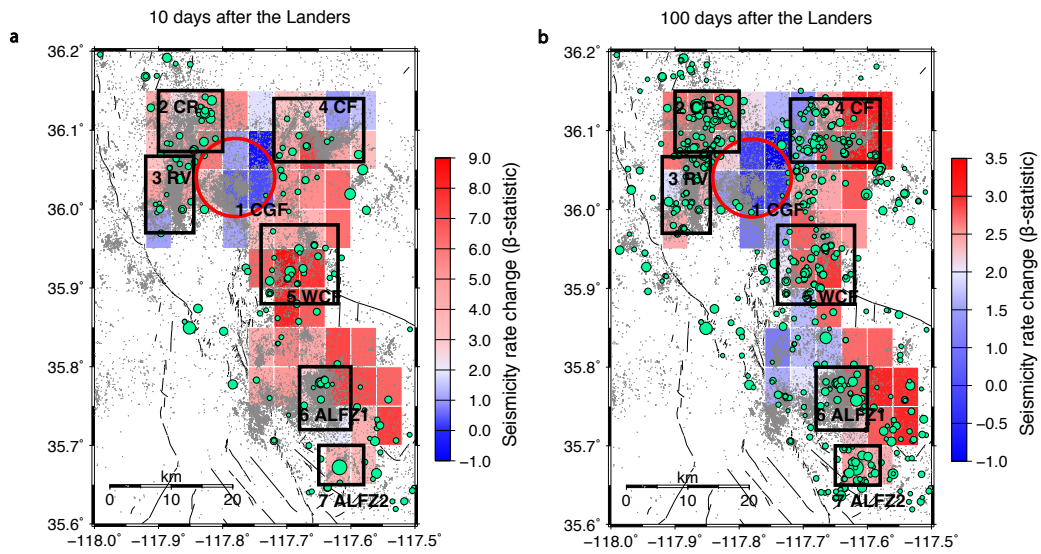


Figure 3. Map views of seismicity rate change between different time windows in the Coso geothermal field and its vicinity. All legends are the same as those in Fig. 2a in the main text, which shows the β -statistic of 30 days after the Landers earthquake relative to the background seismicity (1987-1993). (a) β -statistic of 10 days after the Landers earthquake. (b) β -statistic of 100 days after the Landers earthquake.

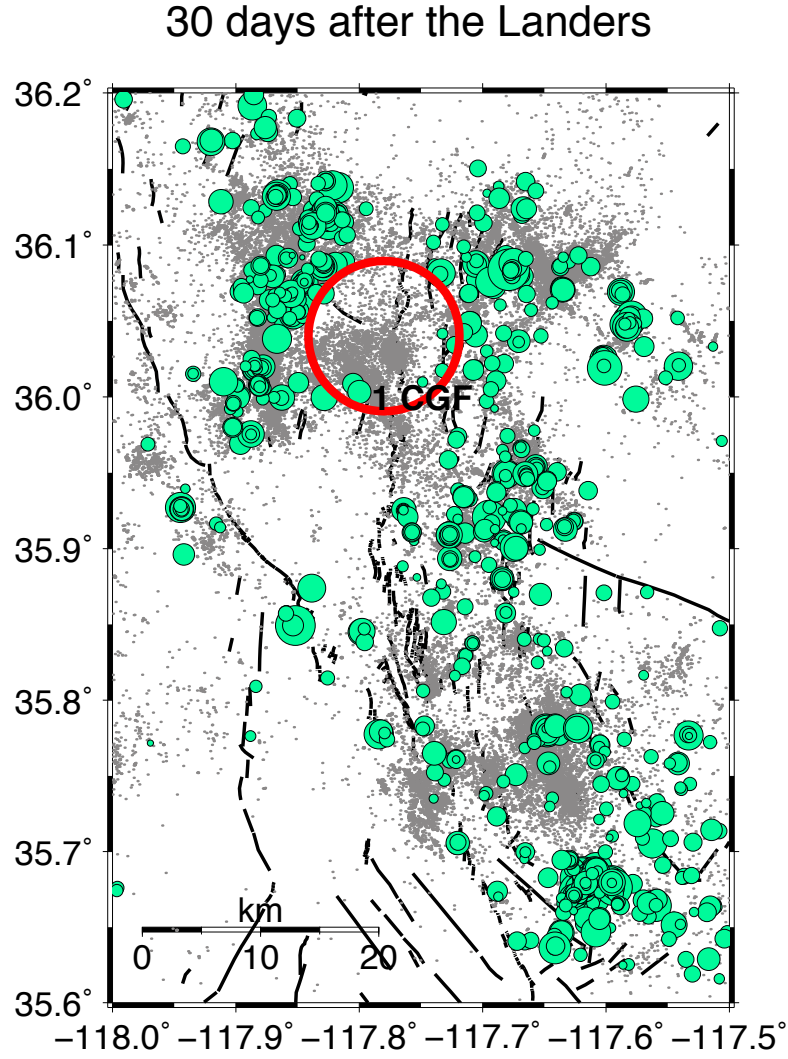


Figure 4. Spatial distribution of seismicity using the raw catalog. Green circles denote seismicity 30 days after the Landers earthquake. Grey dots are the seismicity between 1981 and 2011. The red circle represents the Coso geothermal field.

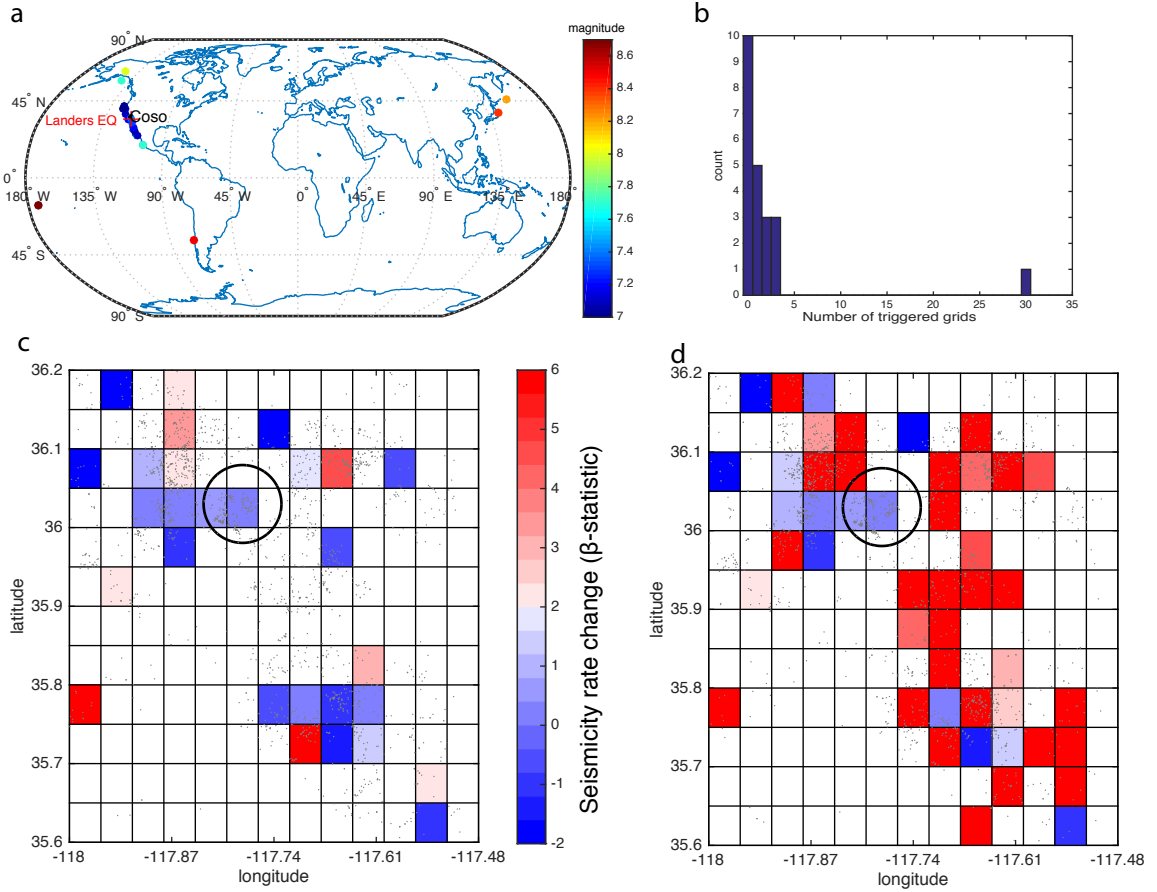


Figure 5. Triggering response of 22 remote earthquakes in the Coso area. (a) Distribution of 22 selected mainshocks. (b) Histogram of triggered grids following the remote mainshocks. The Landers earthquake triggered 30 grids, significantly more than other mainshocks. (c) Stacked map of seismicity rate change following the 21 mainshocks other than the Landers earthquake. The grids are at a scale of $0.04^\circ \times 0.05^\circ$ and are colored by β -values. (d) Stacked map of seismicity change following all the 22 mainshocks. The legends are the same as in (c).

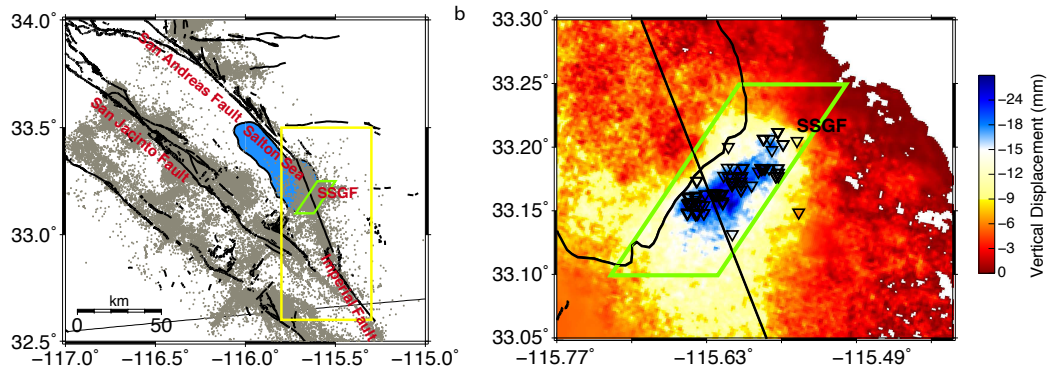


Figure 6. Tectonics and location of the Salton Sea geothermal field (SSGF). Green polygons outline the same location of the SSGF. (a) Tectonic map showing the faults and the background seismicity between 1981 and 2010. Yellow box encloses our entire study area, including the SSGF and its vicinity. The Salton Sea is shown in blue. (b) Locations of injection and extraction wells (black triangles), obtained from the California Oil, Gas, and Geothermal Resources (DOGGR). Background is accumulated subsidence in the SSGF that occurred between 2003 and 2010 from InSAR result (Heresh Fattahi, personal communication, 2014).

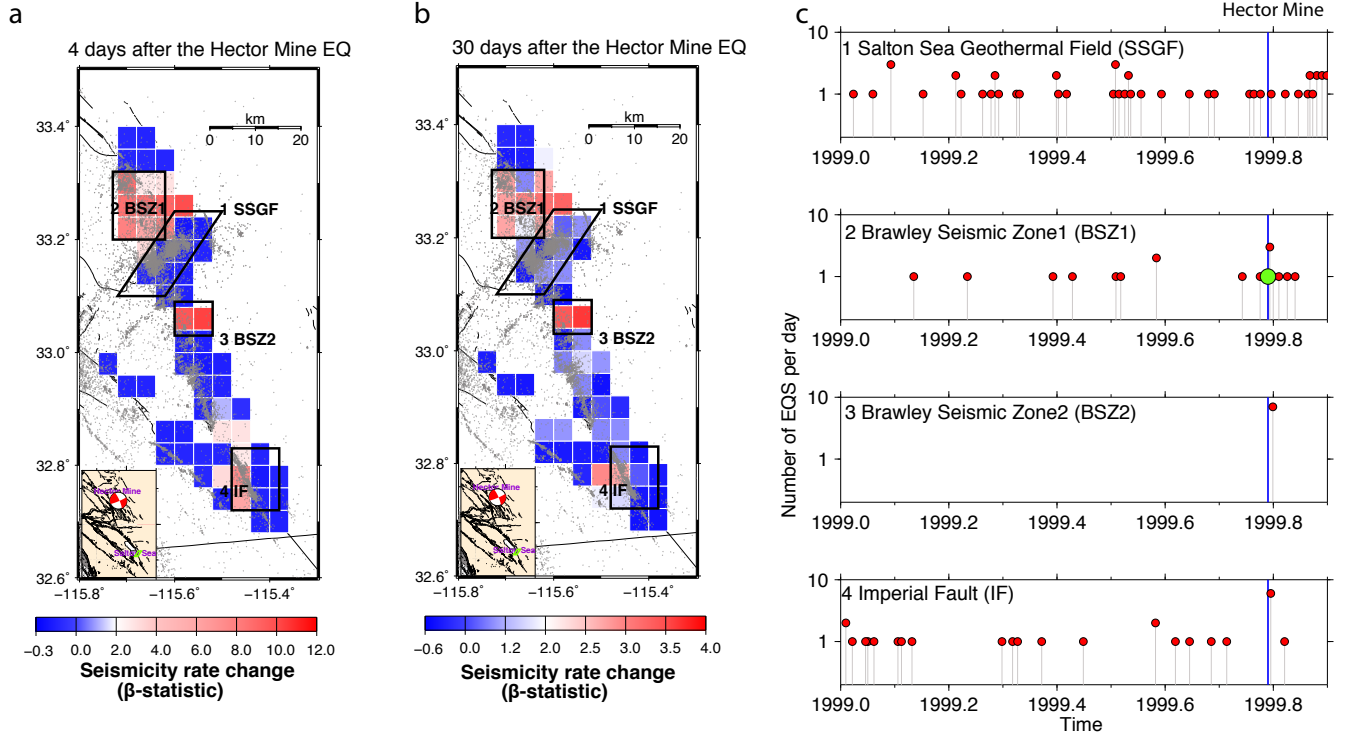


Figure 7. Seismicity rate change in the Salton Sea geothermal field (SSGF) and its vicinity. Map view of β -statistic of 4 days (a) and 30 days (b) after the 1999 Mw 7.1 Hector Mine earthquake relative to the background seismicity (1996-2002). Polygon outlines the SSGF based on the location of the active injection and extraction wells. Boxes mark the subareas outside of the geothermal field, including the Brawley Seismic Zone (BSZ) and Imperial Fault (IF). Grey dots denote the background seismicity from 1981 to 2010. Inset shows the location of the Hector Mine earthquake and the SSGF. (c) One-year time series in the SSGF and its vicinity. The first panel is the SSGF. The other three are the subareas outside the SSGF. Red dots represent microearthquakes with $1.7 \leq M_w < 4.0$ in the declustered catalog and green dots for $M_w \geq 4.0$. Blue line marks the onset of the Hector Mine earthquake.